Biorheology 52 (2015) 235–245
DOI 10.3233/BIR-15058
IOS Press

Histological and biomechanical changes in a mouse model of venous thrombus remodeling

Y.-U. Lee [a], A.Y. Lee [a], J.D. Humphrey [b] and M.K. Rausch [b,*]
[a] *Tissue Engineering Program, Nationwide Children's Hospital, Columbus, OH, USA*
[b] *Department of Biomedical Engineering, Yale University, New Haven, CT, USA*

Received 8 June 2015
Accepted 22 August 2015

Abstract.
BACKGROUND: Deep vein thrombosis and the risk of pulmonary embolism are significant causes of morbidity and mortality. Much remains unclear, however, about the mechanisms by which a venous thrombus initiates, progresses, or resolves. In particular, there is a pressing need to characterize the evolving mechanical properties of a venous thrombus for its mechanical integrity is fundamental to many disease sequelae.
OBJECTIVE: The primary goal of the present study was to initiate a correlation between evolving histological changes and biomechanical properties of venous thrombus.
METHODS: We employed an inferior *vena cava* ligation model in mice to obtain cylindrical samples of thrombus that were well suited for mechanical testing and that could be explanted at multiple times following surgery. Using uniaxial micromechanical testing, we collected stress–stretch data that were then fit with a microstructurally-inspired material model before submitting the samples to immunohistological examination.
RESULTS: We found that venous thrombus underwent a radially inward directed replacement of fibrin with collagen between 2 weeks and 4 weeks of development, which was accompanied by the infiltration of inflammatory and mesenchymal cells. These histological changes correlated with a marked increase in material stiffness.
CONCLUSIONS: We demonstrated that 2 to 4 week old venous thrombus undergoes drastic remodeling from a fibrin-dominated mesh to a collagen-dominated microstructure and that these changes are accompanied by dramatic changes in biomechanical behavior.

Keywords: Venous ligation, intraluminal thrombosis, stiffness, stress, clot

1. Introduction

Deep vein thrombosis (DVT) is a significant source of morbidity and mortality [1,2]. Although many suffer from the consequences of DVT, the mechanisms of initiation, progression, and resolution remain poorly understood. Indeed, particularly scant is information on the evolving mechanical properties of a venous thrombus. Such properties are fundamental to the mechanical integrity of the thrombus, especially its ability to remain intact under hemodynamic loads [3–6]. There is, therefore, a pressing need for more information on thrombus biomechanics.

*Address for correspondence: M.K. Rausch, Department of Biomedical Engineering, Yale University, 55 Prospect Street, New Haven, CT 06511, USA. E-mail: manuel.rausch@yale.edu.

If not proteolytically resolved, venous thrombus can undergo several phases of maturation in which the initial fibrin mesh is infiltrated by inflammatory and mesenchymal cells that gradually lead to a thickening of extant fibrin fibers or replacement with other structural proteins, including collagens [7–9]. Of course, such remodeling and replacement of structural constituents within a thrombus alters its biomechanical properties [5]. Quantitative relationships between changes in composition, organization, and biomechanical properties remain incompletely characterized. Consequently, an improved understanding of venous thrombus remodeling, particularly changes in its nonlinear biomechanical properties, promises to contribute to our understanding of DVT and thereby help clinicians make better-informed decisions about the best course of treatment for their patients.

Because it is difficult to track the remodeling of thrombus in patients and because *in vitro* generated fibrin equivalents tend not to exhibit the stiffness or strength observed for *in vivo* explants [10], several animal models have been introduced to study DVT. For example, Deatrick et al. [11] developed a murine model wherein they ligated the inferior *vena cava* (IVC) to create a space filling thrombus. Notwithstanding the challenge of working with such small vessels, murine models offer the added advantages of diverse genetic manipulations and the wide availability of antibodies.

Although different animal models have increased our understanding tremendously, there has yet to be a correlation of evolving histological changes with biomechanical properties. The primary goal of the present study, therefore, was to initiate such a correlation. We employed the IVC ligation model in mice for it yields a nearly cylindrical thrombus that is amenable both to standard uniaxial mechanical testing and subsequent immunohistological examination. Data collected over 4 weeks of thrombus evolution revealed a progressive remodeling from a fibrin-based towards a fibrin–collagen composite structure that was accompanied by a marked stiffening of the material response. We submit that this murine model holds considerable promise for understanding better the evolving histomechanical properties of venous thrombus.

2. Materials and methods

2.1. Mouse model

All animal protocols were approved by the Yale University Institutional Animal Care and Use Committee. Briefly, we used intraperitoneal injections of ketamine (100 mg/kg) and xylazine (20 mg/kg) to anesthetize ∼8 week old male C57BL/6 mice. While under deep anesthesia, and using aseptic techniques, we surgically exposed and then ligated with 7-0 silk suture the IVC and its major branches just beneath the left renal vein. The incision was then closed and the animal was allowed to recover with appropriate analgesics as well as normal food and drink supplied *ad libitum*. For more details on this type of procedure, see [11,12]. Two and four weeks after surgery, we euthanized the mice with an intraperitoneal injection of Beuthanasia-D. Immediately thereafter, we harvested the IVC containing an intraluminal thrombus and immediately placed samples of 2 mm length or longer in phosphate buffered saline until testing. The wall of the IVC was gently removed, thus leaving a nearly cylindrical sample of intraluminal thrombus for mechanical testing.

2.2. Uniaxial tests

We impaled each end of the thrombus with a custom glass cannula and secured the ends with a drop of cyanoacrylate before mounting them within a custom mechanical testing system [13]. The system com-

prised two precision motors to uniaxially extend the sample in opposing directions, which maintained the center within the same field of view of a video microscope. An axial force transducer recorded the reaction forces while custom software based on an edge-detection algorithm monitored changes in diameter in the sample center. All tests were performed in physiologic solution at 37°C.

Before collecting data for analysis, we preconditioned the specimens by loading them four times from 0 to $10g$. After completing these cycles, we measured the unloaded length and diameter. Thereafter, we loaded each sample twice to a load of $1g$, then twice to $2g$, and so forth up to a $10g$ maximum load. Following this protocol, we removed the samples from the cannulae and fixed them overnight in 10% formalin in the unloaded configuration.

2.3. Histology

Fixed samples were cut into distal and proximal halves, embedded in paraffin, and sectioned at 5 μm thicknesses. Sections from the sample center were stained with Movat's pentachrome to identify fibrin and collagen and with picrosirius red to identify different thickness collagen fibers. Additional sections were immuno-stained for α-smooth muscle actin (αSMA) to identify myofibroblasts, CD68 to identify macrophages and Ly6b to identify neutrophils.

We acquired all histological images with an Olympus BX51TF microscope and an Olympus DP70 camera using bright-field imaging, except for the picrosirius red stained sections, which were acquired using polarizing optics and dark-field imaging. Both bright-field and dark-field images were taken at $10\times$ and $20\times$ magnification. We performed quantitative measurements using ImageJ (NIH) and an in-house Matlab image processing software.

2.4. Mechanical characterization

To quantify the mechanical behavior of the thrombi under cyclic uniaxial loading, we transformed the force-displacement data sets into Cauchy stress–stretch data and attempted to fit the data with several different well established constitutive relations for soft tissues. For each model fit, we assumed the thrombus to be (pseudo)elastic; that is, we ignored any hysteresis remaining after preconditioning and focused on loading cycles alone. Of the models examined, which included standard phenomenological models such as the Fung-exponential, the microstructural model proposed by Hurschler et al. [14] yielded the best fit. Specifically, their model represents the Cauchy stress in the loading direction, $\sigma(\lambda)$, in terms of a convolution integral that embodies a distribution function for the so-called recruitment stretch, $P_w(\lambda_s)$, and the stress-response of the individual microstructural fiber, σ_0. That is,

$$\sigma = \int_{\gamma}^{\lambda} P_w(\lambda_s)\sigma_0(\lambda/\lambda_s)\,\mathrm{d}\lambda_s, \tag{1}$$

where P_w, in turn, is represented by the 3-parameter Weibull distribution function,

$$P_w = \frac{\beta}{\delta}\left(\frac{\lambda_s-\gamma}{\delta}\right)^{\beta-1}\exp\left(-\left(\frac{\lambda_s-\gamma}{\delta}\right)\right)^{\beta}. \tag{2}$$

This distribution function is defined by a shape parameter β, a scaling parameter δ, and a location parameter γ. β and δ determine the shape of the toe region of the material response and γ determines

the shift of the material response along the stretch-axis. In the present case, we approximated the stress-response of an individual microstructural fiber, σ_0, with a standard neo-Hookean material model. Under the assumption of a homogenous, one-dimensional fiber, with no fiber-to-fiber interactions, we write σ_0 in terms of a single material parameter, the shear modulus μ, and the effective fiber stretch $\overline{\lambda} = \lambda/\lambda_s$, namely

$$\sigma_0 = \mu\left(\overline{\lambda}^2 - 1\right). \tag{3}$$

Finally, note that we assumed that the fibers did not have any compressive stiffness. Thus, the integral expression in Eq. (1) describes the material stress response as the sum of infinitesimal tensile stress contributions by each neo-Hookean fiber, individually activated at a recruitment stretch λ_s as prescribed by the recruitment stretch distribution function P_w.

The model parameters were determined via nonlinear regression of the experimental uniaxial data. Specifically, identifications were accomplished using the Levenberg–Marquardt algorithm implemented in Matlab R2013b.

2.5. Statistical analysis

We compared samples at 2 and 4 weeks using the independent, two-tailed student t-test. Furthermore, computed values of material stiffness at 2 and 4 weeks, for all ten loading protocols each, were compared using 2-way ANOVA. Alpha levels for both tests were set to 0.05. All data are reported as means $\pm$ 1 standard deviation unless indicated otherwise.

3. Results

The animal studies yielded an IVC thrombus in 17 mice at the two time points of interest. Of these 17 thrombi, 11 were long enough to be studied under uniaxial extension testing: $n = 5$ in the 2 week group and $n = 6$ in the 4 week group. All tested thrombi had an approximately cylindrical shape. Upon further gross examination, thrombi at 2 weeks appeared pink and slightly translucent (Fig. 1(A) and (C)) whereas those at 4 weeks appeared white and opaque (Fig. 1(B) and (D)); the latter was due, in part, to the 4-week thrombi being covered with fibrous tissue and having integrated partially within the wall of the IVC. There was a trend ($p = 0.19$) toward a greater length at 2 compared to 4 weeks (Fig. 1(E)), perhaps due to a progressive compaction over time. The thrombi diameters were significantly larger ($p < 0.01$) at 2 compared to 4 weeks (Fig. 1(F)).

Staining with Movat's pentachrome revealed an accumulation of fibrin in the center of the thrombi at 2 weeks, which tended to disappear by 4 weeks (Fig. 2(A) and (B)). This qualitative observation was supported by a significant ($p < 0.001$) decrease in the percent area fraction of fibrin from 2 to 4 weeks (Fig. 2(G)). Interestingly, the observed collagen tended to exist primarily along the periphery of the thrombi at 2 weeks, whereas it tended to be distributed throughout the bulk of the thrombi at 4 weeks (Fig. 2(A) and (B)). This observation was supported by the picrosirius red staining, which revealed further that the fibrillar collagen at 2 weeks was loosely organized whereas that at 4 weeks was more compact and distributed throughout the cross-section (Fig. 2(C) and (D)). These trends were revealed, on average, by the quantitative analysis in Fig. 2(H) that shows a significant increase ($p < 0.001$) in the percent area fraction of fibrillar collagen from 2 to 4 weeks. Note, too, the marked transition from 2 to 4 weeks from thinner (green/yellow) to thicker (red/orange) collagen fibers (Fig. 2(C) and (D)).

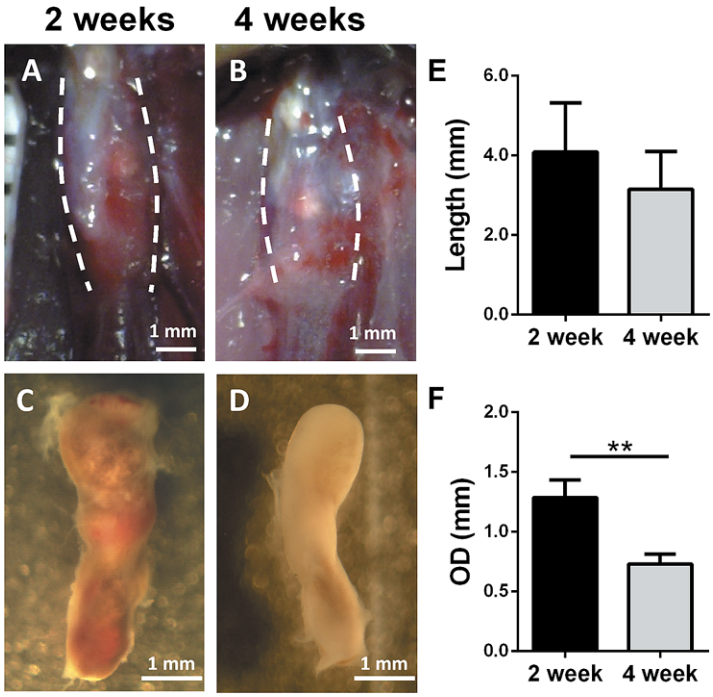

Fig. 1. Remodeling thrombus changes appearance over time from red to white and undergoes contraction. Representative (A), (B) *in situ* images of the inferior *vena cava* containing thrombus (*dashed lines*) and (C), (D) *in vitro* images of thrombus following excision and isolation from the venous wall, both for 2 and 4 weeks post-surgery. Comparison of mean values of isolated thrombus (E) length and (F) outer diameter (OD) at 2 ($n = 5$) and 4 ($n = 6$) weeks post-surgery revealed significant differences. $^{**}p < 0.01$. (Colors are visible in the online version of the article; http://dx.doi.org/10.3233/BIR-15058.)

Staining for αSMA suggested that myofibroblast activity was limited primarily to the periphery of the thrombus at 2 weeks, but this activity transitioned to a more diffuse distribution throughout the thrombus at 4 weeks (Fig. 2(E) and (F)). These distributions of cells corresponded well with the observed distributions of collagen (Fig. 2(C) and (D)). Note, however, that the total area fraction of αSMA did not change between these two times (Fig. 2(I)); the actin-positive cells were merely more distributed. Similar to the (presumed) myofibroblast activity, macrophage and neutrophil activity transitioned from the periphery of the thrombus at 2 weeks to a widespread distribution at 4 weeks (Fig. 3(A)–(D)). In contrast to the myofibroblast activity, cell counts for the macrophages and neutrophils increased significantly ($p < 0.05$) from 2 to 4 weeks (Fig. 3(E) and (F), respectively).

Figure 4(A) and (B) shows images of the central region of a representative sample while mounted within the mechanical testing device and loaded to $0g$ (unloaded reference) or $10g$ (maximum imposed load). The resulting Cauchy stress–stretch data sets for representative thrombus samples at 2 and 4 weeks are shown in Fig. 4, panels (C) and (D), respectively. In both cases, we omit the second loading cycle for each loading step for clarity. These data illustrate the nonlinear character upon loading as well as some hysteresis, which appeared to lessen somewhat at 4 compared with 2 weeks. In addition, a Mullin's type damage phenomenon manifested as a continued shifting to a more extensible behavior upon increasing load. This damage type response was qualitatively similar at 2 and 4 weeks.

As a first step toward correlating changes in tissue organization with changes in mechanical behavior, we evaluated the ability of different Fung-type exponential constitutive relations to fit the observed

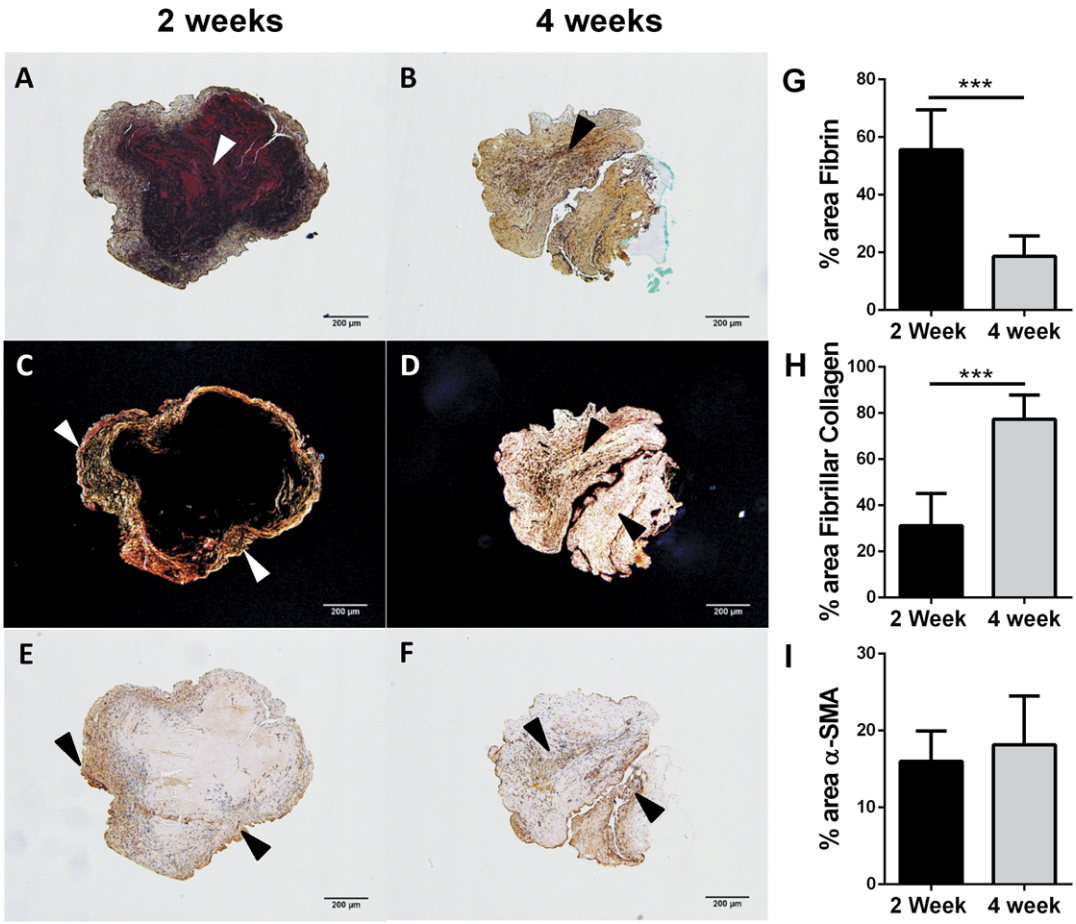

Fig. 2. Remodeling thrombus undergoes replacement of fibrin with collagen from the periphery inwards, while αSMA positive cell number remains nearly constant. (A), (B) Staining with Movat's pentachrome revealed spatio-temporal distributions of fibrin and collagen, (C), (D) while staining with picrosirius red highlighted fibrillar collagens and (E), (F) staining for αSMA identified cells likely to be myofibroblasts. Percent area fractions are compared at 2 and 4 weeks for (G) fibrin, (H) fibrillar collagen and (I) αSMA-positive cell activity. $^{***}p < 0.001$. (The colors are visible in the online version of the article; http://dx.doi.org/10.3233/BIR-15058.)

loading curves under each of the multiple conditions (e.g., loading up to $1, 2, \ldots, 10g$). Although some fits were reasonable, large numbers of parameters were necessary to capture the remarkably flat pre-toe region and nearly linear post-toe region. We next evaluated the ability of a microstructurally-inspired constitutive relation to fit the uniaxial tensile test data; Table 1 summarizes the resulting material parameters. Representative fits to the same stress–stretch data shown in Fig. 4(C) and (D) are illustrated in Fig. 5(A). These data sets highlight the general trend that samples at 4 weeks were notably stiffer (higher stress at the same or lower stretch levels) than samples at 2 weeks. With the use of the microstructurally-inspired material model and identified parameters, we could also derive analytically the material stiffness from the Cauchy stress. Figure 5(B) compares the mean material stiffness at each load level between the 2- and 4-week samples. Generally, mean material stiffness increased both with increasing load and with age. While the former observation was not supported by the ANOVA ($p = 0.076$), increasing material stiffness between 2 and 4 weeks was statistically significant ($p < 0.001$).

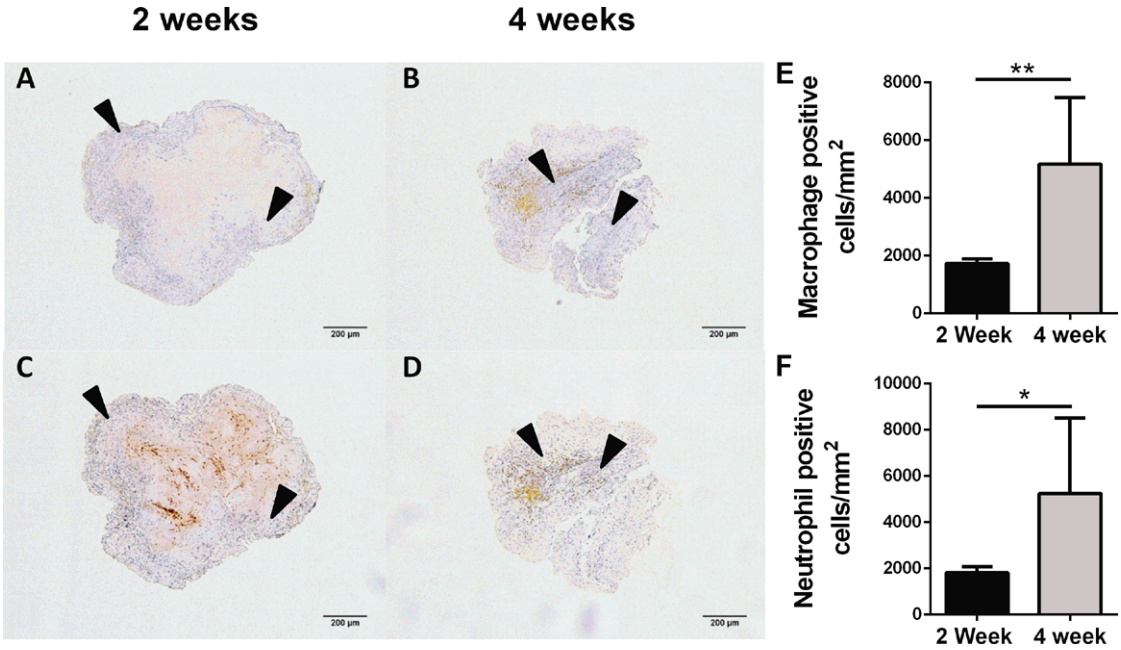

Fig. 3. Macrophages and neutrophils increased in density and invaded the remodeling thrombus from the periphery inwards. (A), (B) CD68 positive staining revealed the presence of macrophages whereas (C), (D) Ly6b positive staining revealed neutrophils. Both cell types increased in concentration from 2 to 4 weeks: (E) CD68 positive cells and (F) Ly6b positive cells. $^{**}p < 0.01$, $^{*}p < 0.05$. (Colors are visible in the online version of the article; http://dx.doi.org/10.3233/BIR-15058.)

4. Discussion

We employed an established *in vivo* mouse model of venous thrombus that naturally yields samples that are convenient for standard mechanical testing without the need to cut or shape the samples. Hence, this model allows one to begin to correlate the evolving composition and mechanical properties while quantifying spatial distributions and concentrations of the different cell types thought to remodel thrombus. Our results, for two times of development, represent the first mechanical characterization of this thrombus model. Preliminary tests revealed that the thrombus was not sufficiently stiff at 1 week post-surgery to permit the collection of robust uniaxial data using our current device; in contrast, data at 2 and 4 weeks post-surgery revealed a dramatic evolution in both composition and material stiffness. Whereas thrombi at 2 weeks consisted primarily of fibrin, with some collagen fibers near the periphery, thrombi at 4 weeks were highly collagenous throughout the cross-section. Indeed, these thrombi sustained extremely high stresses without gross failure (Figs 4 and 5). The infiltration of α-smooth muscle positive cells, presumably myofibroblasts but possibly fibrocytes, into the peripheral regions of the thrombus at 2 weeks but throughout the thrombus at 4 weeks strongly suggests a primary role for these cells in the synthesis and organization of collagen during the radially-directed, inward remodeling process. Similar findings were reported before, though evolving mechanical properties were not reported [7,8,15]. The observed increased deposition of collagen was accompanied by a reduction in thrombus size (Fig. 1), consistent with the phenomenon of wound contraction that is aided by contractile myofibroblasts [16]. Associated increases in neutrophils and macrophages from 2 to 4 weeks suggested, however, that continued thrombus remodeling may still have been driven largely by inflammation at 4 weeks. That macrophages secrete transforming growth factor beta, among many other cytokines, is

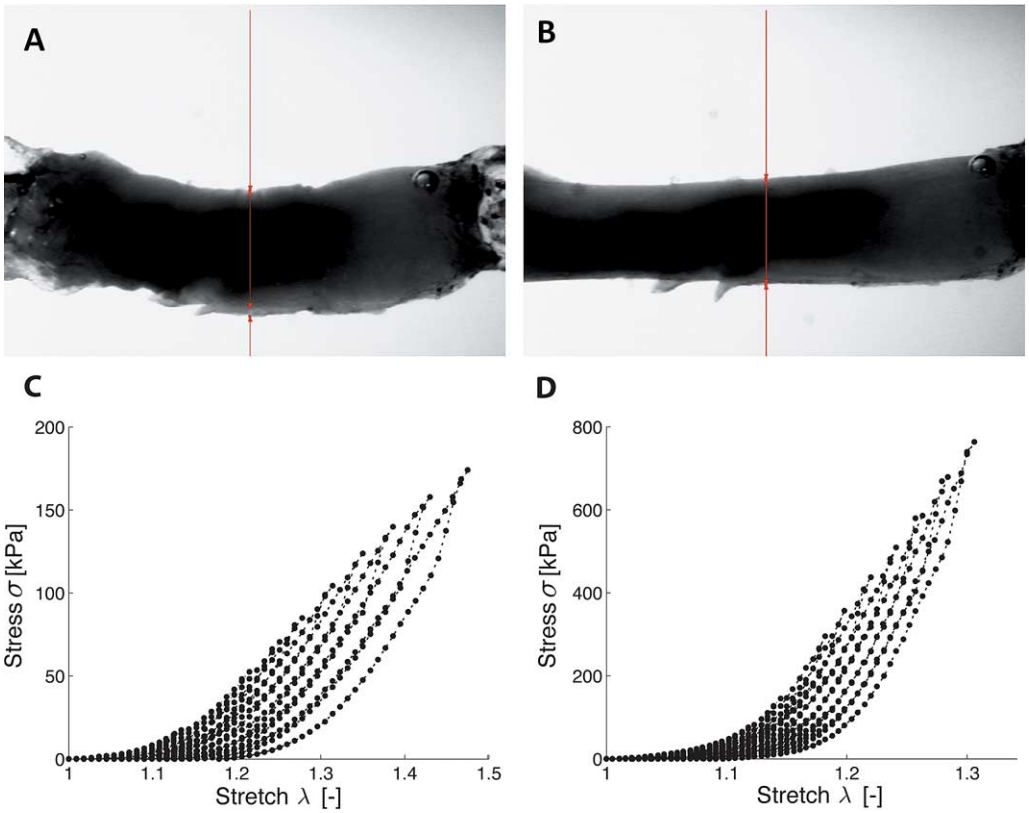

Fig. 4. Thrombus samples exhibited nonlinear uniaxial Cauchy stress–stretch responses, with hysteresis and a Mullin's type damage behavior. Video-capture images during uniaxial testing show representative thrombus geometries at a load of (A) 0g and (B) 10g. Representative cyclic loading data reveal a nonlinear response with hysteresis at (C) 2 weeks and (D) 4 weeks. Note the very different scales, which reflect the marked stiffening at 4 compared with 2 weeks.

consistent with the differentiation of fibroblasts to myofibroblasts under the influence of mechanical stress [17], thus supporting a potentially important paracrine interaction between these two cell types. Although we did not measure fibrin degradation products, the inflammatory cells also likely contributed to the degradation of the fibrin that allowed it to be replaced with collagen. Future studies should explore thrombus remodeling in this model at times beyond 4 weeks.

The material behavior of the thrombi did not change qualitatively between the younger and older samples. Both showed a nonlinear stress–stretch response, with hysteresis and a Mullin's type damage phenomenon that was reflected by notable shifts in the material response along the stretch-axis as the load was increased. Nevertheless, significant quantitative changes in structural composition were accompanied by quantitative changes in mechanical properties from 2 to 4 weeks of development.

To correlate the quantitative changes in mechanical properties with changes in structural composition, we fit the collected stress–stretch data with a number of material models for soft tissue. We found that the microstructurally-inspired material model by Hurschler et al. [14] provided the best fit, with the added benefit of requiring only 4 parameters. Based on this material model and the identified parameters, we were able to derive continuous, analytical expressions not only for Cauchy stress as a function of stretch, but also for the material stiffness. Given these expressions, we found a statistically significant difference in material stiffness between 2 and 4 weeks – with the mean stiffness higher at 4 weeks compared to

Table 1
Parameters of the microstructurally-inspired material model fit to uniaxial tensile test data of thrombus at 2 weeks and 4 weeks for loads from $1g$ to $10g$ (see Eqs (1)–(3))

		$1g$	$2g$	$3g$	$4g$	$5g$	$6g$	$7g$	$8g$	$9g$	$10g$
						Parameter μ					
Mean [kPa]	2 weeks	676.78	506.64	829.84	816.83	861.58	1041.41	944.91	1198.51	1072.89	1111.96
	4 weeks	9987.34	5497.95	7663.11	3028.23	2610.87	2749.21	2933.21	3148.27	3463.15	3341.39
STD [kPa]	2 weeks	792.22	700.04	950.89	453.03	856.95	722.68	976.80	701.13	952.63	1009.64
	4 weeks	10,523.37	4195.18	15,818.29	2919.18	2497.59	2481.07	2565.40	2748.92	3163.00	3419.11
						Parameter β					
Mean [–]	2 weeks	11.25	15.62	21.75	30.04	12.06	15.39	10.76	12.74	7.89	10.96
	4 weeks	15.27	14.85	12.08	16.09	16.05	18.39	15.85	16.05	13.55	12.67
STD [–]	2 weeks	16.99	18.28	28.78	37.05	10.32	7.55	8.67	9.46	8.37	8.20
	4 weeks	7.92	7.87	8.12	4.40	6.83	8.58	5.92	5.63	4.25	8.64
						Parameter γ					
Mean [–]	2 weeks	0.25	0.32	0.37	0.50	0.37	0.49	0.38	0.52	0.37	0.45
	4 weeks	0.60	0.59	0.49	0.59	0.58	0.67	0.64	0.67	0.58	0.49
STD [–]	2 weeks	0.30	0.34	0.28	0.25	0.28	0.19	0.28	0.30	0.29	0.31
	4 weeks	0.50	0.35	0.35	0.09	0.11	0.16	0.13	0.07	0.13	0.33
						Parameter δ					
Mean [–]	2 weeks	0.45	0.38	0.57	0.66	0.58	0.70	0.58	0.72	0.65	0.58
	4 weeks	0.62	0.60	0.52	0.60	0.63	0.56	0.60	0.60	0.49	0.36
STD [–]	2 weeks	0.44	0.35	0.36	0.23	0.37	0.18	0.37	0.27	0.40	0.37
	4 weeks	0.35	0.25	0.31	0.05	0.12	0.17	0.13	0.08	0.07	0.25

Note: Symbols are the shear modulus μ, the shape parameter β, the location parameter γ and the scale parameter δ.

2 weeks for each load level – consistent with the significant change from a fibrin-dominated to collagenous thrombus (cf. Fig. 2). Notwithstanding large specimen-to-specimen variability, as expected of an evolving disease process, the observed increase in mean material stiffness with increasing thrombus age is qualitatively consistent with reports on the mechanical properties of thrombi of various levels of maturity explanted from human AAAs [18]. We emphasize, however, that the present data are the first for a relatively early (weeks rather than years) maturation of a venous, not arterial, clot. Given the goodness of fit provided by the microstructurally-inspired material model, we submit that the model and identified parameters will lend themselves well for future studies of thrombus mechanics in general, though with site-specific values of parameters.

To the best of our knowledge, this is the first time that a Mullin's type damage behavior has been reported for relatively early thrombus. While the observed behavior is not, strictly speaking, the same as the classical Mullin's effect in elastomers, it shows remarkable resemblance [19]. Our finding may nevertheless be of particular interest as this phenomenon could result in damage-induced anisotropy, and perhaps help explain the directionally-dependent material properties that have been reported for intraluminal thrombus in aneurysms [18].

Interestingly, the transition from a fibrin-dominated mesh to a more mature, collagen-dominated network was not accompanied by a quantitative reduction of characteristics that are typically associated with viscoelasticity, including hysteresis and load-history dependence [20,21]. We speculate that the total occlusion of the IVC and associated failure to replenish important coagulation factors from the flowing blood, such as factor VIII, may have prevented complete cross-linking of the fibrin and collagen

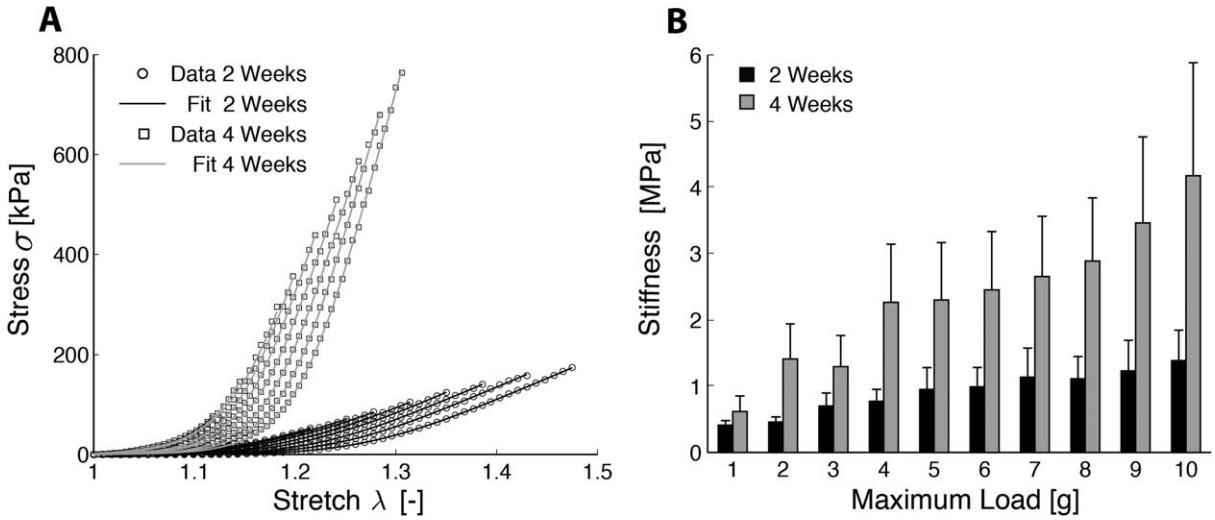

Fig. 5. A microstructurally-inspired material model fit well the loading responses of 2 and 4 week thrombi and revealed that mean material stiffness increased over time and with increasing load in remodeling thrombus. (A) Loading data from representative samples at 2 (*circles*) and 4 (*squares*) weeks post-surgery that were subjected to increasingly greater loads ($1, 2, \ldots, 10g$) were fit-well by the microstructurally-inspired constitutive model. Fits for other samples were similar. (B) Material stiffness was calculated for each sample and each load level as the slope of the stress–stretch curve at maximum stretch. Material stiffness is significantly higher at 4 compared to 2 weeks ($p < 0.001$) and showed an increasing trend with each load level ($p = 0.076$). Data shown as mean $\pm$ 1 standard error of the mean.

fibers within the central region of the thrombus that was tested. Such non-cross-linked meshes have been shown to exhibit pronounced viscoelastic responses [22], as observed here. Thus, thrombi formed under isolated, stagnant flow conditions may present with mechanical properties different from those that form under non-obstructive flow conditions, as, for example, those discussed in [12,23,24]. This limitation should be kept in mind before extrapolating the present mechanical data to thrombi formed under different conditions. Furthermore, thrombi are complex, three-dimensional biomaterials with a heterogeneous microstructure. Importantly, in our current model we assumed that thrombus can be represented by a constrained homogenous mixture, thus our mechanical modeling represents only the bulk behavior of the material, not that of its individual spatially distributed (radially or axially) constituents or their interactions.

5. Conclusion

We showed that an established mouse model of venous thrombus naturally yields specimens that are convenient for uniaxial testing, and thus can be used to correlate histological and biomechanical changes in remodeling thrombus. We demonstrated that 2- to 4-week old thrombus can undergo drastic remodeling from a fibrin-dominated mesh to a collagen-dominated microstructure and that these changes are accompanied by marked increases in stiffness. That a simple microstructurally-inspired constitutive relation described well the associated data suggests that *in vivo* changes could be predicted. There is, however, a need for similar data covering additional times, with quantification of the biomechanics of earlier thrombus (days rather than weeks) remaining a technical challenge due to its extreme compliance.

Acknowledgement

This work was supported, in part, by NIH Grants R03 EB010109, R01 HL086418 and U01 HL116323 to Yale University.

References

[1] Kyrle PA, Eichinger S. Deep vein thrombosis. Lancet. 2005;365:1163–74.
[2] Weinmann EE, Salzman EW. Deep-vein thrombosis. N Engl J Med. 1994;331:1630–41.
[3] Roberts WW, Lorand L, Mackros LF. Viscoelastic properties of fibrin clots. Biorheology. 1973;10:29–42.
[4] Roberts WW, Kramer O, Rosser RW, Nestler FHM, Ferry JD. Rheology of fibrin clots. I. Biophys Chem. 1974;1:152–60.
[5] Emelianov SY, Chen X, O'Donnell M, Knipp B, Myers D, Wakefield TW, et al. Triplex ultrasound: Elasticity imaging to age deep venous thrombosis. Ultrasound Med Biol. 2002;28:757–67.
[6] Karsaj I, Humphrey JD. A mathematical model of evolving mechanical properties of intraluminal thrombus. Biorheology. 2009;46:509–27.
[7] Fineschi V, Turillazzi E, Neri M, Pomara C, Riezzo I. Histological age determination of venous thrombosis: A neglected forensic task in fatal pulmonary thrombo-embolism. Forensic Sci Int. 2009;186:22–8.
[8] Nosaka M, Ishida Y, Kimura A, Kondo T. Time-dependent organic changes of intravenous thrombi in stasis-induced deep vein thrombosis model and its application to thrombus age determination. Forensic Sci Int. 2010;195:143–7.
[9] Schriefl AJ, Collins MJ, Pierce DM, Holzapfel GA, Niklason LE, Humphrey JD. Remodeling of intramural thrombus and collagen in an Ang-II infusion ApoE-/- model of dissecting aortic aneurysms. Thromb Res. 2012;130:e139–46.
[10] Ku DN, Flannery CJ. Development of a flow-through system to create occluding thrombus. Biorheology. 2007;44:273–84.
[11] Deatrick KB, Eliason JL, Lynch EM, Moore AJ, Dewyer NA, Varma MR, et al. Vein wall remodeling after deep vein thrombosis involves matrix metalloproteinases and late fibrosis in a mouse model. J Vasc Surg. 2005;42:140–8.
[12] Diaz JA, Obi AT, Myers DD, Wrobleski SK, Henke PK, Mackman N, et al. Critical review of mouse models of venous thrombosis. Arterioscler Thromb Vasc Biol. 2012;32:556–62.
[13] Gleason RL, Gray SP, Wilson E, Humphrey JD. A multiaxial computer-controlled organ culture and biomechanical device for mouse carotid arteries. J Biomech Eng. 2004;126:787–95.
[14] Hurschler C, Loitz-Ramage B, Vanderby R. A structurally based stress–stretch relationship for tendon and ligament. J Biomech Eng. 1997;119:392–9.
[15] Lee D, Yuki I, Murayama Y, Chiang A, Nishimura I, Vinters HV, et al. Thrombus organization and healing in the swine experimental aneurysm model. Part I. A histological and molecular analysis. J Neurosurg. 2007;107:94–108.
[16] Tomasek JJ, Gabbiani G, Hinz B, Chaponnier C, Brown RA. Myofibroblasts and mechano-regulation of connective tissue remodelling. Nat Rev Mol Cell Biol. 2002;3:349–63.
[17] Hinz B. The myofibroblast: Paradigm for a mechanically active cell. J Biomech. 2010;43:146–55.
[18] Tong J, Cohnert T, Regitnig P, Holzapfel GA. Effects of age on the elastic properties of the intraluminal thrombus and the thrombus-covered wall in abdominal aortic aneurysms: Biaxial extension behaviour and material modelling. Eur J Vasc Endovasc Surg. 2011;42:207–19.
[19] Beatty MF, Krishnaswamy S. A theory of stress-softening in incompressible isotropic materials. J Mech Phys Solids. 2000;48:1931–65.
[20] Humphrey JD. Cardiovascular solid mechanics: Cells, tissues, and organs. New York: Springer; 2002.
[21] Van Dam EA, Dams SD, Peters GWM, Rutten MCM, Schurink GWH, Buth J, et al. Determination of linear viscoelastic behavior of abdominal aortic aneurysm thrombus. Biorheology. 2006;43:695–707.
[22] Münster S, Jawerth LM, Leslie BA, Weitz JI, Fabry B, Weitz DA. Strain history dependence of the nonlinear stress response of fibrin and collagen networks. Proc Natl Acad Sci. 2013;110:12197–202.
[23] Kamada H, Tsubota K, Nakamura M, Wada S, Ishikawa T, Yamaguchi T. Computational study on effect of stenosis on primary thrombus formation. Biorheology. 2011;48:99–114.
[24] Von Brühl ML, Stark K, Steinhart A, Chandraratne S, Konrad I, Lorenz M, et al. Monocytes, neutrophils, and platelets cooperate to initiate and propagate venous thrombosis in mice in vivo. J Exp Med. 2012;209:819–35.